Iranian J Biotech. 2018 July;16(3):e1684 **DOI:10.15171/ijb.1684**

Research Article

Genome-Scale Metabolic Network Models of Bacillus Species Suggest that Model Improvement is Necessary for Biotechnological Applications

Tahereh Ghasemi-Kahrizsangi, Sayed-Amir Marashi *, Zhaleh Hosseini

Department of Biotechnology, College of Science, University of Tehran, Tehran, Iran.

**Corresponding author*: Sayed-Amir Marashi. Department of Biotechnology, College of Science, University of Tehran, Tehran, Iran.

Phone: +98-21-66491622, Ext. 105; E-mail: marashi@ut.ac.ir

Received: 1 Aug. 2016; **Revised**: 7 Sep. 2017; **Accepted**: 18 Sep. 2017; **Published online:** 11 Aug. 2018

Background: A genome-scale metabolic network model (GEM) is a mathematical representation of an organism's metabolism. Today, GEMs are popular tools for computationally simulating the biotechnological processes and for predicting biochemical properties of (engineered) strains.
Objectives: In the present study, we have evaluated the predictive power of two GEMs, namely *i*Bsu1103 (for *Bacillus subtilis* 168) and *i*MZ1055 (for *Bacillus megaterium* WSH002).
Materials and Methods: For comparing the predictive power of *Bacillus subtilis* and *Bacillus megaterium* GEMs, experimental data were obtained from previous wet-lab studies included in PubMed. By using these data, we set the environmental, stoichiometric and thermodynamic constraints on the models, and FBA is performed to predict the biomass production rate, and the values of other fluxes. For simulating experimental conditions in this study, COBRA toolbox was used.
Results: By using the wealth of data in the literature, we evaluated the accuracy of *in silico* simulations of these GEMs. Our results suggest that there are some errors in these two models which make them unreliable for predicting the biochemical capabilities of these species. The inconsistencies between experimental and computational data are even greater where *B. subtilis* and *B. megaterium* do not have similar phenotypes.
Conclusions: Our analysis suggests that literature-based improvement of genome-scale metabolic network models of the two *Bacillus* species is essential if these models are to be successfully applied in biotechnology and metabolic engineering.

Keywords: Biochemical capability; Bacillus Species; Computational biotechnology; Model validation; Systems biology.

1. Background

Advances in genome sequencing in the last decades have made it possible to reconstruct genome-scale metabolic network models (GEMs) for many organisms (1-6). Over recent years, the number of available metabolic networks has significantly increased in different taxa of living organisms (7-13). Nowadays, analysis of GEMs plays an indispensable role in metabolic engineering (14, 15).

The process of GEM reconstruction is comprised of four fundamental steps (6, 16) including: automated omics-based (mainly genomics-based, i.e., using the sequenced genome of organisms) reconstructing the draft network using toolboxes such as COBRA toolbox (17) or RAVEN toolbox (18); curating the draft reconstruction; converting the network to a computational model and finally evaluating the correctness of models using experimental data.

In the process of GEM reconstruction, metabolic data of an organism is collected, and then, converted into a machine readable format, which in turn is converted to a mathematical constraint-based model. In fact, GEMs can be seen as the mathematical representation of metabolic processes. In the Materials and Methods section, we will briefly explain the mathematical framework used in this study.

In spite of the great advances in the reconstruction of GEMs (19), current models may not be completely

successful in modeling experimental data. Such inconsistencies may occur due to incorrect or incomplete annotations, missing reactions and pathways, incorrect or missing regulatory constraints and inaccurate formulation of the biomass reaction (14, 20).

As a result of the potential deficiencies in GEMs, it is always necessary to validate a GEM to ensure its ability in predicting the behavior of organism (21). In a recent comparative study, we assessed the modeling capabilities of GEMs of three Pseudomonas species, namely, *P. aeruginosa*, *P. putida* and *P. fluorescens* (22). Using the previously published biochemical data, we showed that GEMs of *P. aeruginosa* and *P. putida* are much more accurate than the *P. fluorescens* GEM.

2. Objectives

In the present study, we follow a similar idea. Two *Bacillus* species, namely *B. subtilis* and *B. megaterium* are chosen for this analysis. The goal of this work is to compare the computationally-modeled biochemical capabilities of these species with their *in vivo* biochemical capabilities.

3. Materials and Methods

3.1.Comprehensive Literature Searching for Experimental Data

For comparing the predictive power of GEMs, experimental data were obtained from previous wet-lab studies. For this purpose, we considered all articles in PubMed database, containing the names of the two species of interest. By June 2014, searching for "*Bacillus subtilis*" AND "*Bacillus megaterium*" in PubMed database resulted in 610 articles. These articles were carefully investigated to check whether they are appropriate for evaluating the *in silico* experiments.

In selecting the articles for evaluation, a number of criteria were considered. Firstly, only those articles which include data on metabolic activities of the two species were chosen. Secondly, we considered only those *in vivo* experiments which are related to the metabolic activities present in both of the two GEMs. For example, different growth rates in the same growth medium and the ability of bacteria in consuming/producing a special substance are appropriate results for evaluating simulations. Metabolic engineering of *B. subtilis* and *B. megaterium* could have been ideal for evaluating simulations. However, we could not find cases of simultaneous engineering of both species.

3.2. Genome-Scale Metabolic Network Models

In the present study, two genome-scale metabolic network models were used: (i) the GEM of *B. subtilis* 168 (called *i*Bsu1103) (23); and (ii) the GEM of *B. megaterium* WSH002 (called *i*MZ1055) (24).

3.3. Flux Balance Analysis of Metabolic Networks

For mathematical representation of metabolism, an $m \times n$ stoichiometric matrix (**S**) is used. In this matrix, rows and columns represent the system's metabolites and reactions, respectively. Element S_{ij} is the stoichiometric coefficient of metabolite i in reaction j. The fluxes of all reactions are represented in vector **v** with the length of n. Now, consider vector **c** as an m-dimensional vector of metabolite concentrations. Then, one can show that $\mathbf{S}.\mathbf{v} = d\mathbf{c}/dt$ holds for the metabolic network (25).

For a system at steady-state conditions, no net production or consumption of metabolites is possible, which means that $d\mathbf{c}/dt = \mathbf{0}$. Consequently, at steady-state conditions, flux through each reaction is given by the stoichiometric constraint, i.e. $\mathbf{S}.\mathbf{v} = \mathbf{0}$. In addition to the stoichiometric constraint, vector **v** is also limited because of thermodynamic or environmental constraints. These constraints limit each flux v_i between a lower bound and an upper bound, in the form $a_i \leq v_i \leq b_i$. In the especial case of irreversible reaction i, flux through the reaction is limited by the thermodynamic constraint $0 \leq v_i$.

Flux balance analysis (FBA) (25) is a computational technique based on linear programming. The aim of FBA is to find the optimal solution of an objective function (typically biomass production rate) subject to stoichiometric, thermodynamic and environmental constraints. For this purpose, the stoichiometric and thermodynamic constraints are extracted from a GEM, while the environmental constraints should be defined depending on the growth medium (See section 3.4.).

3.4. COBRA Toolbox for in Silico Analyses

For simulating experimental conditions in this study, COBRA toolbox was used (17). This toolbox contains various functions which can be used for performing a variety of *in silico* metabolic network analyses, including FBA.

For simulating a specific experiment, *in vivo* growth medium conditions were applied to models. For example, the uptake rate of all those metabolites which were absent in the medium were set to zero. On the other hand, the uptake rates of the constituents of the medium were constrained between zero and an upper bound value. After setting the environmental, stoichiometric and thermodynamic constraints, FBA is

performed to predict the biomass production rate, and the values of other fluxes.

Similar to some of the previous studies (26, 27), the most frequently used functions in this study are explained below:

- "changeRxnBounds" can be used to modify lower or upper bounds of a reaction. Using this function, environmental constraints can be simulated.
- In some cases it was needed to have a reaction which was not included in the models. In these situations "addReaction" was used. The input of this function is the chemical equation of the reaction. The function adds reactions to the metabolic model.
- After applying the desired conditions to the models, FBA should be performed (using "optimizeCbModel" function) to predict the growth phenotypes in a certain growth medium.

4. Results

4.1. Utilization of Amino Acids as the Sole Source of Carbon and Nitrogen

Consuming single L-amino acids as the only source of carbon and nitrogen is a common phenomenon amongst prokaryotes and occurs in most genera of bacteria (28-30). Metabolism of amino acids by bacteria has been widely studied. For example, in a comprehensive study, twenty taxonomically known bacteria (including *B. subtilis* and *B. megaterium*), which can utilize amino acids, were examined for their growth capabilities on amino acids (31). In this study, utilization of twenty amino acids was examined (among which utilization pattern of ten amino acids was found to be different in *B. subtilis* and *B. megaterium*).

In each experiment, Lochhead-Chase basal medium (32) was used, in which glucose and nitrate were replaced by a certain single amino acid. Moreover, this medium contains mineral salts. Since the exact constituents of this medium could not be determined, we performed the *in silico* simulations in mineral salt medium (MSM) which includes mineral salts. MSM medium contains the following salts: K_2HPO_4, KH_2PO_4, $(NH_4)_2SO_4$, $MgCl_2$, $CaCl_2$, H_3BO_3, $ZnSO_4$, $NiSO_4$, $(NH_4)_6Mo_7O_{24}.4H_2O$, $CuSO_4.5H_2O$, $MnSO_4$, $CoCl_2$, and $FeCl_3$. As our goal is to simulate the amino acid as the single source of carbon and nitrogen, we did not consider NH_4 in our simulated media.

For simulating this experiment, we defined the mentioned medium for models. This was done by setting the lower bound of uptake reaction for desired ions to -10 millimoles per gram dry weight per hour ($mmol.gDW^{-1}.hr^{-1}$). Additionally, the lower bounds of glucose and nitrate uptake rates were set to zero. In each of the simulations, we set the lower bound of the uptake rate of a certain amino acid to -10 $mmol.gDW^{-1}.hr^{-1}$. By this process, we defined each amino acid as the single source of carbon and nitrogen. Uptake reactions of Hydroxyproline and Cystine were not included in the two GEMs, and therefore, FBA was not carried out for these amino acids.

In **Table 1**, *in silico* growth results are compared to the experimental *in vivo* data for differentially-consumed amino acids in the two species. In this table and also in **Table 2**, the terms "good growth" and "poor growth" refers to the experimental data. We have also differentiated between these two groups in calculation of Kendall rank coefficients which are reported below. From these data, *in vivo* biomass production in either *B. megaterium* or *B. subtilis* can be observed, while, in many cases, *in silico* simulations fail to predict such differences. In other words, there is no significant correlation between experimental and computational

Table1. *In silico* and *in vitro* data of amino acid utilization of differentially-consumed patterns in *B. Megaterium* and *B. Subtilis*. Relative cell growth estimated visually from the amount of growth on the amino acid. ++: Good growth; + : Poor growth; − : No growth.

Amino Acids	*Bacillus subtilis*		*Bacillus megaterium*	
	***In vitro* data**	***In silico* data ($mmol.gDW^{-1}.hr^{-1}$)**	***In vitro* data**	***In silico* data ($mmol.gDW^{-1}.hr^{-1}$)**
Valine	++	0.6608	−	0.8423
Isolucine	++	0.8820	−	1.0602
Serine	+	0.3056	−	0.3807
Threonine	+	0.4520	−	0.4774
Aspartic acid	−	0.3862	++	0.4676
Arginine	++	0.7423	−	0.8841
Histidine	+	0.6772	++	0
Tryptophan	+	0	−	0

Table 2. *In silico* and *in vivo* data of amino acid utilization with similar consumption patterns in *B. megaterium* and *B. subtilis*. Relative cell growth estimated visually from the amount of growth on the amino acid. ++: Good growth; +: Poor growth; −: No growth.

Amino acids	*Bacillus subtilis*		*Bacillus megaterium*	
	***In vivo* data**	***In silico* data (mmol.gDW^{-1}.hr^{-1})**	***In vivo* data**	***In silico* data (mmol.gDW^{-1}.hr^{-1})**
Glycine	−	0.1055	−	0.2180
Alanine	++	0.3670	++	0.4405
Leucine	−	0	−	0
Cysteine	−	0	−	0
Methionine	+	0	+	0
Glutamic acid	++	0.6007	++	0.7175
Lysine	+	0	+	0
Phenylalanine	−	0	−	0
Tyrosine	−	0	−	0
Proline	++	0.7206	++	0.8303

results (Kendall rank coefficient of 0.56 (p-value = 0.07) and -0.38 (p-value = 0.24) for *B. subtilis* and *B. megaterium* respectively).

In the same study (31), utilization patterns of ten amino acids were found to be similar in *B. subtilis* and *B. megaterium*. *In silico* and *in vivo* growth rates for these amino acids are compared in Table 2. Here, unlike Table 1, the two GEMs successfully predicted the *in vivo* results in most cases including the utilization of alanine, leucine, cysteine, glutamic acid, phenylalanine, tyrosine and proline (Kendall rank coefficient of 0.62 for *B. subtilis* and *B. megaterium,* p-value < 0.05). These results suggest that in case of similar phenotypes, the responsible reactions/pathways are also included in both GEMs.

4.2. Carbohydrate Fermentation Capability

A recent analysis has been conducted to study the diversity of a chlorine-resistant Bacillus population isolated from a wastewater treatment station (33). This study has investigated the phenotypic and genotypic diversity of this bacterial population. Based on 16S rRNA gene sequencing and biochemical tests, 12 strains were identified. Similarity searches on GenBank showed that five of these strains were *Bacillus subtilis*, while one strain was identified as *Bacillus megaterium* (33).

One of the biochemical tests done in this experiment was the carbohydrate fermentation test. This test was done to investigate the acid and gas production during carbohydrate utilization in bacteria. Growth medium used in this test includes $NH_4H_2PO_4$, KCl, $MgSO_4$, Bromothymol blue and carbohydrate of interest.

For simulating this experiment, we proposed that when a strain is capable of growing on a carbohydrate source, it may or may not be able to produce acid (i.e., to ferment the carbohydrate). This means a correct positive result in the *in silico* analysis might have equivalent negative or positive result in the *in vivo* experiment. However, if the strain cannot use the carbohydrate as source of carbon and energy, the result of its fermentation test must necessarily be negative, as it cannot use the carbohydrate.

For modeling fermentation, in each simulation we set a carbohydrate to be the sole source of carbon/energy, and then, FBA was performed. The results are shown in **Table 3**. Interestingly, in all three cases of the first three carbohydrates (D-glucose, D-mannitol, and L-arabinose) the results of simulation are not inconsistent with experimental data.

In the same study (33), the ability of these bacteria in utilizing citrate as single source of carbon has been examined. According to the experimental data, none of those two bacteria was able to grow on citrate. However, *in silico* growth phenotype of *B. megaterium* and *B. subtilis* showed inconsistency with *in vivo* data, i.e., both strains could grow on citrate.

4.3. Effect of Formaldehyde on the Growth of Bacillus Species

Formaldehyde is an antimicrobial compound used as disinfectant against microbial vegetative cells and spores. This compound can inactivate bacteria, fungi, yeasts and molds. In one study, the minimal inhibitory effect of formaldehyde against several bacteria including *Bacillus subtilis* and *Bacillus megaterium* has been measured (34). According to this article, *Bacillus megaterium* was more resistant than *Bacillus subtilis* against formaldehyde. Formaldehyde resistance

Table 3. *In silico* growth phenotypes vs. *in vivo* fermentation phenotypes. +: Positive result; −: Negative result; −/+: Both results have been observed. It should be noted that in case of D-glucose, D-mannitol and L-arabinose, *in silico* data show biomass production from the carbon source, while i*n vivo* data suggest acid production as a result of fermentation. Therefore, inconsistency is guaranteed only when growth is not reported *in silico* but acid production is reported *in vivo*. In case of using citrate as the carbon source, *in silico* results of both GEMs showed inconsistency with *in vivo* results.

Carbohydrate	*Bacillus subtilis*			*Bacillus megaterium*		
	***In silico* data**	***In vivo* data**	**Consistent?**	***In silico* data**	***In vivo* data**	**Consistent?**
D-Glucose	+	−/+	yes	+	+	yes
D-Mannitol	+	−/+	yes	+	−	yes
L-Arabinose	+	−	yes	+	+	yes
Citrate as carbon source	+	−	no	+	−	no

in these two closely-related species is presumably due to the detoxification mechanisms imbedded in their metabolism (35, 36).

For simulating formaldehyde resistance, spontaneous uptake reaction of formaldehyde was added to the two GEMs. Then, in each model, we increased the flux of formaldehyde in a stepwise manner until biomass production rate became zero, or formaldehyde uptake rate reached its upper limit. The results of this study for *Bacillus subtilis* and *Bacillus megaterium* are shown in **Figures 1A and 1B**, respectively.

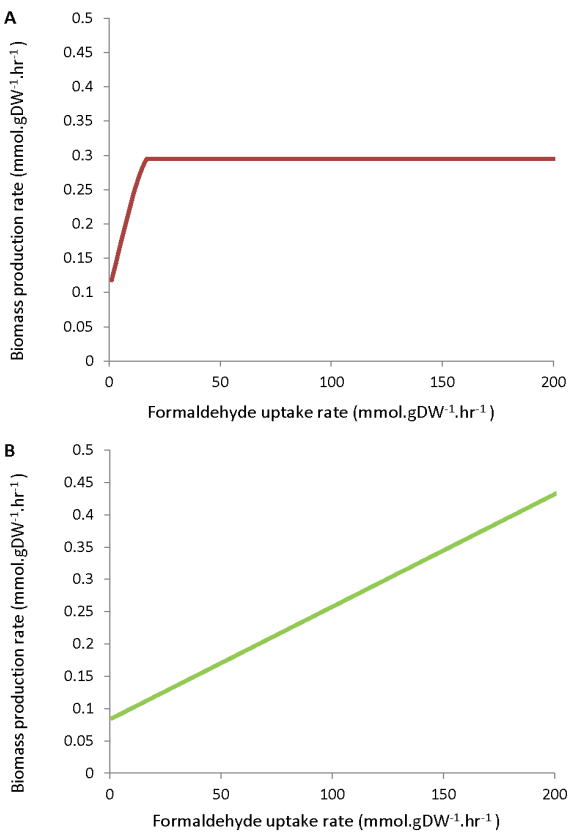

Figure 1. *In silico* biomass production rate as a function of formaldehyde uptake rate in (A) *Bacillus subtilis* and (B) *Bacillus megaterium*

As it is shown in the graphs, not only the biomass production rates do not decrease by formaldehyde uptake flux, but also the biomass production rates increase in both models. In case of *B. subtilis*, biomass production rate gets its maximum value (i.e., 0.295 mmol.gDW^{-1}.hr^{-1}) when formaldehyde uptake becomes 15.8 mmol.gDW^{-1}.hr^{-1} or higher. However, in *Bacillus megaterium*, by increasing formaldehyde uptake flux to 1000 mmol.gDW^{-1}.hr^{-1} biomass production rate persistently increases.

5. Discussion

In this work, we showed that *in silico* simulations fail to predict the differences in the amino acid metabolism of *B. subtilis* and *B. megaterium*. In other words, the two GEMs cannot accurately show the differences in amino acid utilization phenotypes. This might be due to the difference between strains used for *in vivo* experiments and GEM reconstruction. However, such discrepancies might also reflect the poor quality of the two GEMs.

The cases of five amino acids, namely valine, isoleucine, serine, threonine and arginine, should be studied in more details. For these amino acids, *B. megaterium* GEM incorrectly predicts growth, while *in silico* and *in vivo* data of *B. subtilis* are consistent. One possible explanation for this inconsistency is that the *B. megaterium* strain used for GEM reconstruction has much more metabolic capabilities compared to the *B. megaterium* strain used in the *in vivo* studies. However, a stronger possibility is that the *B. megaterium* GEM includes additional

reactions which are not, in reality, in its metabolism. Note that *B. subtilis* GEM had been used as a reference during the reconstruction of *B. megaterium* GEM (24). Therefore, some reactions/pathways which are present in *B. subtilis* but are actually absent in the metabolism of *B. megaterium* might have been wrongly included in its GEM. Such reactions are either needed for filling the gaps of the model and making it functional or present in the model as a mistake of the method used for model reconstruction. Such pathways can be responsible for these observed false positive growth phenotypes.

Based on Table 3, we observe that in case of glucose, mannitol and arabinose, the two GEMs show the capability to use these compounds as carbon source. Consequently, one cannot draw any conclusion on the correctness of the predictions based on the fermentation studies. Furthermore, in case of growth on citrate, *in silico* growth phenotype of *B. megaterium* and *B. subtilis* showed inconsistency with *in vivo* data, i.e., both strains could grow on citrate. Again, these inconsistencies might be either due to difference in strains used for *in vivo* experiments and *in silico* simulations or due to the poor quality of the GEMs.

Therefore, both models failed to reflect the sensitivity of bacteria to formaldehyde. Although one of the reasons for this failure is that metabolic models cannot predict the inhibitory effects, there must be definitely something wrong with the reactions of these models, which caused this failure. In other words, according to their metabolic models, these bacteria have evolved some pathways for consuming formaldehyde as a source of carbon and converting it to biomass precursors. Clearly, this is not reasonable and is probably because of the existence of extra reactions, or reactions with wrong directionalities in these models.

Figure 2A depicts a part of formaldehyde metabolism in the GEM of *B. subtilis*. According to this pathway, formaldehyde is eventually converted to CO_2,

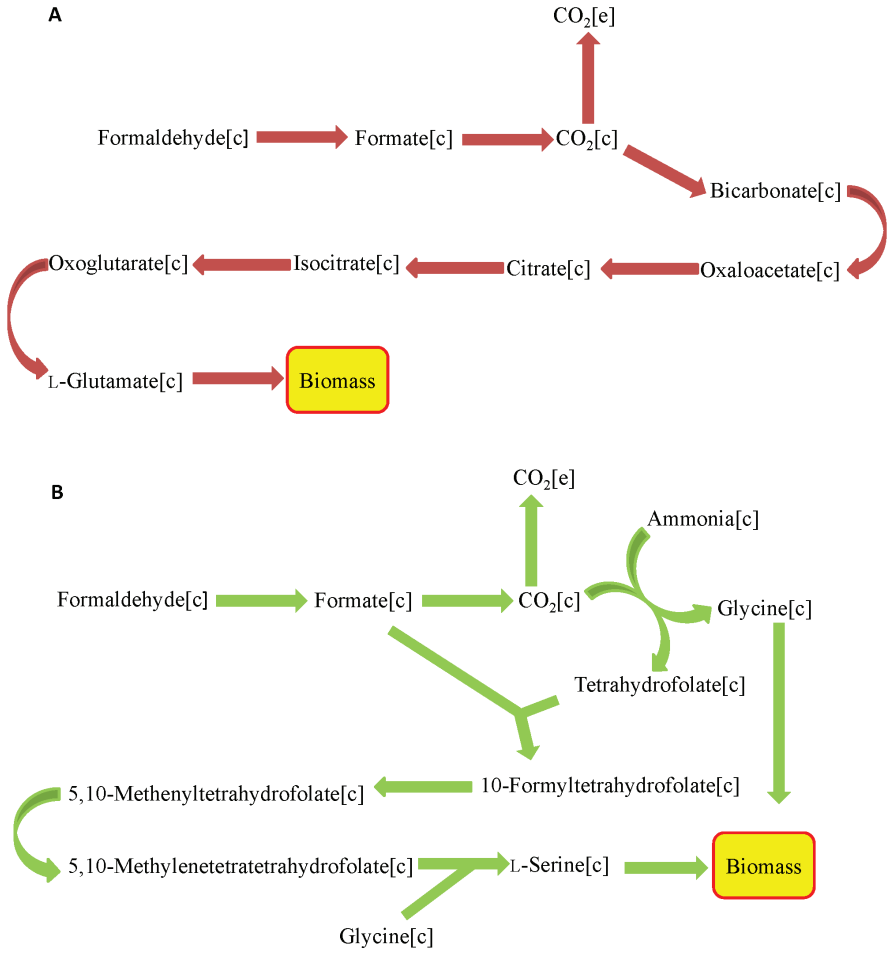

Figure 2. Schematic representation of formaldehyde metabolism according to the A) *Bacillus subtilis* GEM and (B) *Bacillus megaterium* GEM.

bicarbonate, and then to oxaloacetate, which is in turn used for glutamate production. Note that conversion of CO_2 to oxaloacetate is not thermodynamically favorable in a cell. Glutamate is a constituent of biomass. Therefore, in simulation, it is logical that increasing formaldehyde flux lead to increase in biomass.

Figure 2B shows a part of formaldehyde metabolism in the GEM of *B. megaterium*. According to this figure, formaldehyde is converted to formate, and then to CO_2. The model suggests that CO_2, then, reacts with ammonia to produce glycine and tetrahydrofolate. Note that this reaction cannot readily occur in the cell, as it is not thermodynamically favorable. The latter compound can be converted to serine. Note that both glycine and serine are constituents of biomass. Therefore, it is logical for this model not to show formaldehyde inhibitory effect.

6. Conclusion

In the present paper, we compared the predictive power of two genome-scale metabolic networks. The results of such comparison can be used to improve the accuracy of GEMs. The striking result is that, in many of the cases *B. subtilis* and *B. megaterium* GEMs fail to accurately predict the experimental data, especially where the phenotypes the two species are different. Consequently, one can conclude that these metabolic network models have some errors that should be subject to a gap filling process. In other words, further modifications should be performed based on literature reports and experimental results, before these models can be used in metabolic engineering and biotechnological applications.

In the present paper, and also in the sister paper (22), we showed how the wealth of data in the literature can be used for evaluating the accuracy of a genome-scale metabolic network model. We previously showed that, as expected, consolidated reconstruction of metabolic networks of *P. aeruginosa* and *P. putida* reduces the inconsistencies between *in silico* and *in vivo* data. On the other hand, independently reconstructed GEMs should be used with care because of their (potentially extensive) errors in predicting experimental phenotypes. Altogether, we recommend that available literature data can be used for GEM evaluation. Although using such data may not be ideal (e.g., due to strain dissimilarities within the same species), it can reduce the massive time, cost and effort requirements for experimental evaluations (for example see (37)).

Here, we emphasize that *P. fluorescens* GEM (i.e., *i*SB1139) (38) and *B. megaterium* GEM (i.e., *i*MZ1055) (24) failed to accurately predict the experimental phenotypes in many cases. This is a serious concern, as these two models are among the most recently reconstructed GEMs (both are published in 2013). This observation suggests that reconstructing GEMs cannot be considered as a mature field, in spite of using advanced bioinformatics tools. Still, quality and completeness of GEMs highly depend on more reliable procedures, such as extensive manual curation (39).

Another important point should be noted here. Classification of bacterial species highly depends on the differences in the biochemical capabilities. It was previously suggested that the GEM reconstruction will revolutionize prokaryotic systematics (40) by characterizing the metabolic differences. One of our goals in the present study was to check whether the differences in the biochemical capabilities are predictable by the existing GEMs. However, the results are generally disappointing. With such poor results, one should not expect the existing GEMs to correctly predict the phenotype of an organism, let alone the between-species differences in the biochemical capabilities. Additionally, it was recently shown that a high degree of similarity exists among many GEMs, regardless of their phylogenetic relationships (39). Finally, it should be noted that even for a well-defined and reliable genome-scale model, different alternative optimal solutions are expected to occur (41). For all these reasons, exploiting GEMs for phylogenetic reconstruction is far from reality at the moment, and it requires enormous improvements in GEM reconstruction in the first place.

Acknowledgments

We would like to thank P. Babaei (Chalmers University of Technology) for her helpful discussions and all of her help during the initial phase of this study.

References

1. Covert MW, Schilling CH, Famili I, Edwards JS, Goryanin II, Selkov E, *et al*. Metabolic modeling of microbial strains in silico. *Trend Biochem Sci*. 2001;**26**: 179-186.doi: 10.1016/s0968-0004(00)01754-0
2. Edwards JS, Covert M, and Palsson BØ. Metabolic modelling of microbes: the flux-balance approach. *Environ Microbiol*. 2002;**4**:133-140. doi: 10.1046/j.1462-2920.2002.00282.x
3. Reed JL and Palsson BØ. Thirteen years of building constraint-based in silico models of *Escherichia coli. J Bacteriol.* 2003;**185**:2692-2699. doi: 10.1128/jb.185.9.2692-2699.2003
4. Kim TY, Sohn SB, Kim YB, Kim WJ, and Lee SY. Recent advances in reconstruction and applications of genome-scale metabolic models. *Current Opinion Biotechnol*. 2012;**23**: 617-623. doi: 10.1016/j.copbio.2011.10.007
5. Durot M, Bourguignon P-Y, and Schachter V. Genome-scale models of bacterial metabolism: reconstruction and applications. *FEMS Microbiol Rev*. 2009;**33**: 164-190. doi: 10.1111/j.1574-6976.2008.00146.x
6. Feist AM, Herrgård MJ, Thiele I, Reed JL, and Palsson BØ. Reconstruction of biochemical networks in microorganisms.

Nature Rev Microbiol. 2009;**7**:129-143. doi: 10.1038/nrmicro1949
7. Feist AM, Henry CS, Reed JL, Krummenacker M, Joyce AR, Karp PD, *et al*. A genome-scale metabolic reconstruction for *Escherichia coli* K-12 MG1655 that accounts for 1260 ORFs and thermodynamic information. *Mol Syst Biol*. 2007;**3**:121. doi: 10.1038/msb4100155
8. Heinemann M, Kümmel A, Ruinatscha R, and Panke S. In silico genome-scale reconstruction and validation of the *Staphylococcus aureus* metabolic network. Biotech Bioengineering. 2005;**92**:850-864. doi: 10.1002/bit.20663
9. Schilling CH, Covert MW, Famili I, Church GM, Edwards JS, and Palsson BØ. Genome-scale metabolic model of *Helicobacter pylori* 26695. *J Bacteriol*. 2002;**184**:4582-4593. doi: 10.1128/jb.184.16.4582-4593.2002
10. Feist AM, Scholten J, Palsson BØ, Brockman FJ, and Ideker T. Modeling methanogenesis with a genome-scale metabolic reconstruction of *Methanosarcina barkeri*. *Mol Syst Biol*. 2006;**2**:2006.0004.doi: 10.1038/msb4100046
11. Duarte NC, Becker SA, Jamshidi N, Thiele I, Mo ML, Vo TD, *et al*. Global reconstruction of the human metabolic network based on genomic and bibliomic data. *PNAS*. 2007;**104**:1777-1782.doi: 10.1073/pnas.0610772104
12. Quek L-E and Nielsen LK. On the reconstruction of the *Mus musculus* genome-scale metabolic network model. *Genome Informatics*. 2008;**21**:89-100. doi: 10.1142/9781848163324_0008
13. de Oliveira Dal'Molin CG, Quek L-E, Palfreyman RW, Brumbley SM, and Nielsen LK. AraGEM, a genome-scale reconstruction of the primary metabolic network in Arabidopsis. *Plant Physiol*. 2010;**152**:579-589. doi: 10.1104/pp.109.148817
14. Zomorrodi AR, Suthers PF, Ranganathan S, and Maranas CD. Mathematical optimization applications in metabolic networks. *Metabolic Engineering*. 2012;**14**:672-686. doi: 10.1016/j.ymben.2012.09.005
15. Xu C, Liu L, Zhang Z, Jin D, Qiu J, and Chen M. Genome-scale metabolic model in guiding metabolic engineering of microbial improvement. *App Microbiol Biotech*. 2013;**97**:519-539. doi: 10.1007/s00253-012-4543-9
16. Palsson BØ. Systems Biology: Properties of Reconstructed Networks. 2006, Cambridge University Press. doi: 10.1017/cbo9780511790515
17. Schellenberger J, Que R, Fleming RM, Thiele I, Orth JD, Feist AM, *et al.* Quantitative prediction of cellular metabolism with constraint-based models: the COBRA Toolbox v2. 0. *Nat Protocols*. 2011;**6**:1290-1307. doi: 10.1038/nprot.2011.308
18. Agren R, Liu L, Shoaie S, Vongsangnak W, Nookaew I, and Nielsen J. The RAVEN toolbox and its use for generating a genome-scale metabolic model for *Penicillium chrysogenum*. *PLoS Comput Biol*. 2013;**9**(3):e1002980. doi: 10.1371/journal.pcbi.1002980
19. Hamilton JJ and Reed JL. Software platforms to facilitate reconstructing genome-scale metabolic networks. *Environ Microbiol*. 2014;**16**:49-59. doi: 10.1111/1462-2920.12312
20. Kim J and Reed JL. Refining metabolic models and accounting for regulatory effects. *Curr Opin Biotechnol.* 2014;**29**:34-38. doi: 10.1016/j.copbio.2014.02.009
21. Price ND, Reed JL, and Palsson BØ. Genome-scale models of microbial cells: evaluating the consequences of constraints. *Nat Rev Microbiol*. 2004;**2**:886-897. doi: 10.1038/nrmicro1023
22. Babaei P, Ghasemi-Kahrizsangi T, and Marashi S-A. Modeling the differences in biochemical capabilities of *Pseudomonas* species by flux balance analysis: how good are genome-scale metabolic networks at predicting the differences? Scientific World J. 2014;**2014**:416289. doi: 10.1155/2014/416289
23. Oh Y-K, Palsson BØ, Park SM, Schilling CH, and Mahadevan R. Genome-scale reconstruction of metabolic network in *Bacillus subtilis* based on high-throughput phenotyping and gene essentiality data. *J Bioll Chem*. 2007;**282**:28791-28799. doi: 10.1074/jbc.m703759200
24. Zou W, Zhou M, Liu L, and Chen J. Reconstruction and analysis of the industrial strain *Bacillus megaterium* WSH002 genome-scale in silico metabolic model. *J Biotech*. 2013;**164**:503-509. doi: 10.1016/j.jbiotec.2013.01.019
25. Orth JD, Thiele I, and Palsson BØ. What is flux balance analysis? *Nature Biotech*. 2010;**28**:245-248. doi: 10.1038/nbt.1614
26. Aung HW, Henry SA, and Walker LP. Revising the representation of fatty acid, glycerolipid, and glycerophospholipid metabolism in the consensus model of yeast metabolism. *Ind Biotech*. 2013;**9(**4):215-228. doi: 10.1089/ind.2013.0013
27. Gallardo R, Acevedo A, Quintero J, Paredes I, Conejeros R, and Aroca G. In silico analysis of *Clostridium acetobutylicum* ATCC 824 metabolic response to an external electron supply. *Bioprocess Biosyst Eng*. 2016;**39**(2):295-305. doi: 10.1007/s00449-015-1513-5
28. Hamilton R and Greenfield L. The utilization of free amino acids by marine sediment microbiota. *Zeitschrift für Allgemeine Mikrobio*l. 1967;**7**:335-342. doi: 10.1002/jobm.19670070502
29. Jensen DE and Neidhardt FC. Effect of growth rate on histidine catabolism and histidase synthesis in *Aerobacter aerogenes*. *J Bacteriol*. 1969;**98**:131-142
30. Bell SC and Turner JM. Bacterial catabolism of threonine. Threonine degradation initiated by L-threonine-NAD+ oxidoreductase. *Biochem J*. 1976;**156**:449-458. doi: 10.1042/bj1560449
31. Halvorson H. Utilization of single L-amino acids as sole source of carbon and nitrogen by bacteria. *Can J Microbiol*. 1972;**18**:1647-1650. doi: 10.1139/m72-255
32. Lochhead A and Chase F. Qualitative studies of soil microorganisms: V. Nutritional requirements of the predominant bacterial flora. *Soil Sci*. 1943;**55**:185-196. doi: 10.1097/00010694-194302000-00007
33. Paes FA, Hissa DC, Angelim AL, Pinto NW, Grangeiro TB, and Melo VM. Diversity of a chlorine-resistant Bacillus population isolated from a wastewater treatment station. *Water Environ Res*. 2012;**84**:274-281. doi: 10.2175/106143012x13280358613462
34. Trujillo R and Lindell KF. New formaldehyde base disinfectants. *Appl Microbiol*. 1973;**26**:106-110
35. Huyen NTT, Eiamphungporn W, Mäder U, Liebeke M, Lalk M, Hecker M, *et al*. Genome-wide responses to carbonyl electrophiles in *Bacillus subtilis*: control of the thiol-dependent formaldehyde dehydrogenase AdhA and cysteine proteinase YraA by the MerR-family regulator YraB (AdhR). *Mol Microbiol*. 2009;**71**:876-894. doi: 10.1111/j.1365-2958.2008.06568.x
36. Yasueda H, Kawahara Y, and Sugimoto S-i. Bacillus subtilis yckG andyckF Encode Two Key Enzymes of the Ribulose Monophosphate Pathway Used by Methylotrophs, and yckH Is Required for Their Expression. *J Bacteriolog*. 1999;**181**:7154-7160.
37. Kjeldsen KR and Nielsen J. In silico genome-scale reconstruction

and validation of the *Corynebacterium glutamicum* metabolic network. *Biotech Bioengin*. 2009;**102**:583-597. doi: 10.1002/bit.22067

38. Borgos SE, Bordel S, Sletta H, Ertesvåg H, Jakobsen Ø, Bruheim P, *et al*. Mapping global effects of the anti-sigma factor MucA in *Pseudomonas fluorescens* SBW25 through genome-scale metabolic modeling. *BMC Syst Biol*. 2013;**7**:19. doi: 10.1186/1752-0509-7-19
39. Monk J, Nogales J, and Palsson BØ. Optimizing genome-scale network reconstructions. *Nature Biotech*. 2014;**32**:447-452. doi: 10.1038/nbt.2870
40. Barona-Gómez F, Cruz-Morales P, and Noda-García L. What can genome-scale metabolic network reconstructions do for prokaryotic systematics? *Antonie van Leeuwenhoek*. 2012;**101**:35-43. doi: 10.1007/s10482-011-9655-1
41. Motamedian E and Naeimpoor F. Flux distribution in *Bacillus subtilis*: inspection on plurality of optimal solutions. *Iran J Biotechnol*. 2011;**9**:260-266.